RSC Advances

Photonic welding of Ultra-long Copper Nanowire Network for Flexible Transparent Electrodes using White Flash Light Sintering

Journal:	*RSC Advances*
Manuscript ID	RA-ART-12-2015-025548.R1
Article Type:	Paper
Date Submitted by the Author:	22-Dec-2015
Complete List of Authors:	Koduru, Mallikarjuna; Hanyang University, Institute of Nanoscience and Technology Hwang, Hyun-Jun; Hanyang University Chung, Wan Ho; Hanyang University, Department of Mechanical Convergence Engineering Kim, Hak-Sung; Hanyang University, Department of Mechanical Engineering
Subject area & keyword:	Nanomaterials - Nanoscience < Nanoscience

Journal Name

ARTICLE

Photonic welding of Ultra-long Copper Nanowire Network for Flexible Transparent Electrodes using White Flash Light Sintering

K. Mallikarjuna[a,b], Hyun-Jun Hwang[a], Wan-Ho Chung[a],Hak-Sung Kim[a,b,*]

eceived 00th January 20xx,
Accepted 00th January 20xx

DOI: 10.1039/x0xx00000x

www.rsc.org/

Copper nanowire (Cu NW)-based flexible transparent electronics represent an enormous breakthrough for the development of efficient, scalable and facile processing techniques. From the standpoint of commercialization, a cost-effective and eco-friendly procedure for welding nanowires is imperative to fabricate Cu NW network-based transparent electrodes. In this study, a photonic welding method using a white flash light (WFL) technique was developed *in-house* for welding Cu NWs in order to produce highly conductive and transparent electrodes under ambient conditions. Flexible Cu NW films with sheet resistances of 128 Ω/□ and transmittances of > 95% at 560 nm on PET substrates were obtained by using light intensity of 1.0 J/cm^2 with single pulse and an irradiation time of 5 ms. The WFL technique facilitates localized surface heating and subsequent welding at the junction of the Cu NWs with excellent stability, low sheet resistance and no damage to the polymer substrates. It is expected that the WFL technique will be widely applied to flexible printed and optoelectronic devices such as touch panel displays and solar cells.

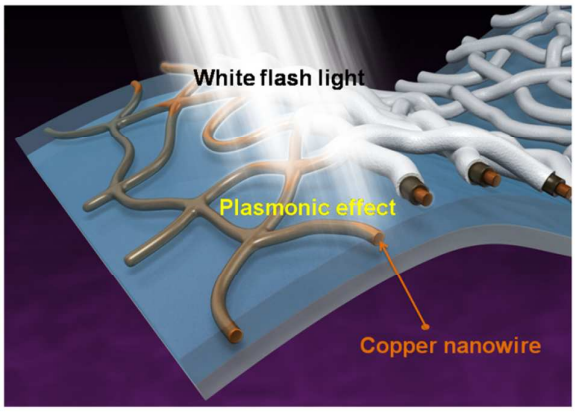

Introduction

Recently, the market for ITO (indium tin oxide)-free flexible transparent conducting electrodes has significantly expanded for usage in flat touch panels of liquid crystal displays (LCDs), organic light emitting diodes (OLEDs), photovoltaic cells, smart phones and tablets; conventional ITO must be replaced due to its brittleness and high cost.[1-4] Several materials such as conducting polymers, carbon nanotubes (CNTs), graphene, metal oxide nanowires and silver nanowires have been explored as potential candidates for replacement of ITO in flexible transparent electrodes.[5-7] For commercialization, it is important to realize low-cost, large-area fabrication, a high transmittance of over 90 % and a sheet resistance lower than 100Ω/□ simultaneously.[8-11] However, among such candidates, conducting polymers are not yet matured for commercialization owing to their relatively high price and high electrical resistance.[12] Transparent electrodes based on graphene and CNT networks have high electrical resistance at high transmittance.[13] Besides, metal and metal oxide nanowire networks with Ag, TiO_2, Al-ZnO, ZnO and MoO_3 form probable alternatives to conventional ITO.[14-16] However, the most critical limitation of these alternative oxides is lack of achieving the required standards of flexible transparent electrodes due to their low conductivity, low transmittance and inherent brittleness.[17] For flexible electronics, any new material has to fulfil a number of criteria in terms of cost and fabrication processes in addition to the usual requirements of the optical transmittance and the electrical conductivity. Under these circumstances, Cu NWs have received the increased attention as an alternative material for flexible transparent electrodes, because of their high conductivity, high transmittance, and low cost.[18] Furthermore, Cu NW-based transparent electrodes are pertinent to large area fabrication of flexible electrodes, which is very important for the anticipated movement towards the flexible electronics.

To achieve high transmittance and low sheet resistance, it is crucial to have low contact resistance at the junctions between the nanowires.[19] In order to attain a low contact resistance, appropriate assembly and contacting procedures are essential to assemble metallic nanowires into large interconnected networks. In this regard, Garnett et al. used a plasmonic welding process to connect silver nanowires. They irradiated light on the silver nanowire, and the silver nanowires were welded together due to plasmonic phenomena.[20] They could achieve 80% transmittance and a 10 Ω/□ sheet resistance. However, silver nanowires are still too expensive to compete with conventional ITO. The prices of Ag NW transparent

[a] Department of Mechanical Engineering, Hanyang University, Haengdang-dong, Seongdong-gu, Seoul 133-791, South Korea
[b] Institute of Nano Science and Technology, Hanyang University, Seoul, 133-791, South Korea
†Electronic Supplementary Information (ESI) available:

electrodes are similar to those of ITO (735 $ per kg) due to the high price of Ag itself (500 $ per kg).[21, 22] For the economic viability, cheaper nanowires (NWs) are required for commercialization.

Cu NW-based flexible electrodes have been receiving immense attention as an alternative to Ag NWs for optoelectronic devices due to their high conductivity and low cost.[23,24] Nevertheless, Cu NW networks have their own drawbacks such as weak bonding between NWs and rapid oxidation that results in the reduced mechanical and electrical stability.[25, 26] The rapid oxidation of Cu NW has been considered to be the critical obstacle preventing their use in applications because inert or reducing gas is needed during the sintering and welding process, which makes the fabrication process complicated and expensive. Moreover, the oxide shells that form on Cu NWs are difficult to be eliminated under ambient conditions using conventional sintering methods like mechanical pressing, conventional thermal sintering, plasma sintering, and microwave sintering.[27, 28] To overcome these limitations, Han et al. developed a plasmonic laser welding process for Cu NWs that selectively heats the NW junction by plasmonic-nanowelding.[29] However, this approach cannot be used for mass production because the laser sintering process can cover only a small sintering area, and the system requires a sophisticated 3D-gantry system in order to cover a large area.

To overcome these limitations, we previously developed a flash light sintering method combined with PVP functionalized copper nanomaterials (Cu NP-inks).[30-36] The white flash light (WFL) method has manifold advantages; (i) WFL sintering method can cover a large area, (ii) short processing time around 10^{-3} seconds using a flash light, (iii) WFL sintering method can be applied to flexible polymer substrate without any damage on the substrates, and (iv) no requirement for maintaining an inert-gas atmosphere. For these reasons, we applied white flash light (WFL) to Cu NWs welding in this work.

We adopted *in-house* developed white flash light sintering method for welding of ultra-long Cu NW networks. Large-area, high percolation conductive transparent electrodes based on Cu NW ink were fabricated on flexible polyethylene terephthalate (PET) substrates using vacuum filtration. The network of Cu NWs was welded at room temperature under ambient conditions in a few milliseconds without damaging the substrate using white flash light (WFL) from a xenon lamp. Upon WFL exposure, photonic sintering produces a large-area welded metal nanostructure network by the photothermal effect. This method can be used to control the electrical conductivity for high transmittance networks, which can be advantageously used for optoelectronic devices.

Experimental

Synthesis of Cu NWs

Copper chloride dihydrate ($CuCl_2.2H_2O$), D-(+) glucose, hexadecylamine (HDA), ethanol, hexane and isopropyl alcohol (IPA) were obtained from Sigma-Aldrich and were used without further purification. Ultra-long Cu NWs were synthesized using a modified wet synthetic approach.[37] First, 50 mg of copper precursor and 280 mg of HDA were added to 20 ml of deionized water and the resultant solution was sonicated in vial using an ultrasonicator for 15 min until a pale blue emulsion was formed. Then, 100 mg of glucose was added and the emulsion was subjected to stirring for 30 min at 55 °C. Thereafter, the vial was capped and sealed with paraffin tape, and the sealed vial was heated in an oven at 102 °C for 6 hours. Upon completion of the reaction, the solution displayed a dark red-brown color, as shown in Figure S1 (Supplementary material), which indicated the formation of Cu NWs. The synthesized Cu NWs were washed with ethanol, hexane and IPA, and the purified Cu NWs were stored in IPA.

Preparation of Cu NW-based transparent electrode

Transparent conducting electrodes (TCEs) with different sheet resistances were prepared using a vacuum filtration method. In a typical preparation, Cu NW ink in IPA was placed in a filtration reservoir, and a 47 mm diameter membrane filter with a pore size of 0.45 µm was attached to the reservoir. Vacuum was applied downstream of the filter to capture the Cu NW percolation network on the membrane filter. The resulting Cu NW network can be transferred to any targeted substrate without using adhesive by placing the Cu NW network against a desired substrate and applying pressure against the membrane filter. The membrane filter was subsequently removed, and the Cu NW network was dried at room temperature, resulting in a transparent conductive electrode with a thickness of 150 µm. The resistivity was controlled by modifying the density of the Cu NWs network by using different quantities of the Cu NW solution for network formation on PET substrates. This formation of network was mainly driven by the applied pressure, vander Waals forces between the Cu NWs and capillary forces between the stabilizers and solvents used during the fabrication procedure.

White flash light system

The WFL sintering system was composed of a xenon flash lamp (PerkinElmer QXA, UK), an aluminium reflector, a power supply, capacitors, a simmer triggering pulse controller and a light filter.[38] WFL was produced using an arc plasma phenomenon in a xenon flash lamp. During arc plasma generation, the lamp emits photons that cover a wide range of wavelengths from 380 nm to 1.0 µm, as shown in Figure 1. This wavelength region covers the absorption spectra of Cu NWs. The WFL generated energy ranged from 1 J/cm^2 to 3 J/cm^2 and was controlled by controlling the number of pulses and the intensity of the arc plasma.

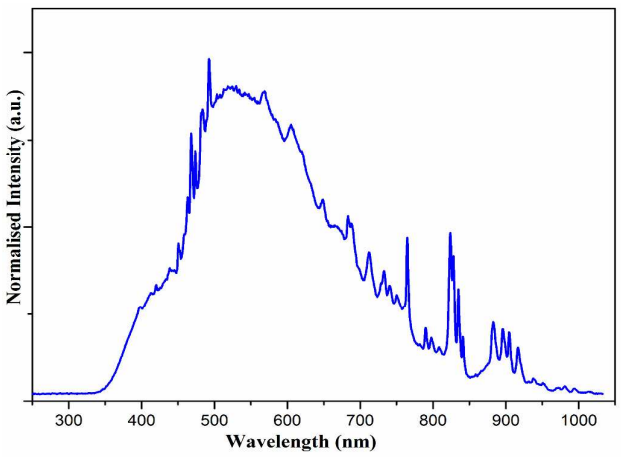

Figure 1: Spectral distribution of flash light from xenon flash lamp.

Characterization

Transparent electrodes were fabricated using an Advantec glass vacuum filtration system with a W2V10 vacuum pump. The optical transmission of the electrodes was measured using a Biochrom Libra S50 UV-Vis spectrophotometer operating at a resolution of 1 nm. The PET substrate was used as a reference. The particle shape, size, distribution and morphology of the Cu NWs were examined using optical and electron microscopes (SEM, S4800Hitachi model and JEM 2100F TEM). X-ray diffraction (XRD) analyses of the thin films were conducted using a D/MAX RINT 2000 (Rigaku) instrument operating in the Bragg-Brentano geometry with Cu Kα radiation (1.540 Å).IR spectra were obtained using a Thermo-Nicolet IR 200 spectrophotometer operated at a resolution of 4 cm^{-1} in the region of 4000-400 cm^{-1}. The sheet resistances of the Cu NWs electrodes were measured using a four-point probe method with a source meter (2611A, Keithley).

Results and discussion

During the synthesis of Cu NWs, amphiphilic molecules containing a cationic head group and an alkyl chain can be used to form various morphological structures such as spheres, hexagonal rods, nanowires, nano tadpoles, nanocubes and polyhedral shapes.[39] HDA is an amphiphilic molecule containing a polar $-NH_2$ group and a non-polar alkyl chain ($-(CH_2)_{15}-CH_3$) that can form various anisotropic structures such as nanowires, rods and cubes.[40-43] In this process, the use of HDA which can react with the copper ion to form the stable intermediate $[Cu(HDA)_2]^{2+}$ is critical for the formation of the Cu NWs. The possible chemical reaction producing the Cu NWs:

$$(Cu(HDA)2)^{2+} + 4OH^- + 2C_5H_{11}O_5\text{-}CHO \longrightarrow Cu + 2HDA + 2H_2O + 2C_5H_{11}O_5\text{-}COOH$$

The amine groups of HDA allow it to bind onto the surface of copper nanostructures in solution. If HDA binds preferentially to the side facets of the Cu NWs, this could cause preferential growth along the axial [110] direction. Finally, the interaction between the functional groups in the alkyl shell and the surface of the copper core was accomplished via a simple one pot reaction.[44] The size, shape and morphology of the as-prepared Cu NWs were determined using microscopy. Clean and continuous Cu NWs network were observed in optical microscopy images shown in Figure S2 (supplementary material), which indicate that the length of NWs varies from tens to hundreds of micrometers; some of NWs were as long as several millimeters.

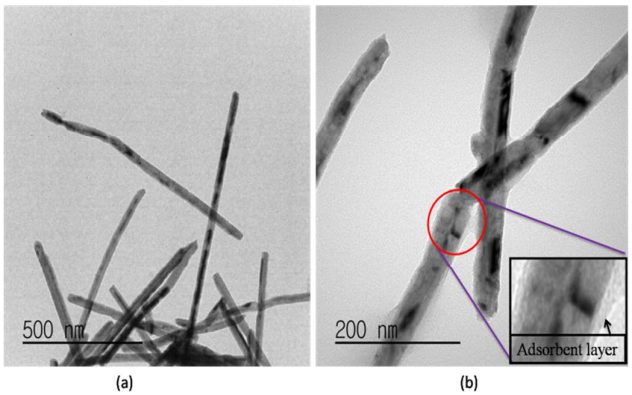

Figure 2: Low and high magnification TEM images of typically synthesized Cu NWs (Inset of the figure shows the adsorbent layer of HDA on Cu NW surface).

It is evident from TEM images (Figure 2) that the Cu NWs were covered with an absorbed layer of HDA with a thickness of 3±1 nm and had a diameter of 36±6 nm. The dark contrast suggests Cu crystals with larger mass thickness in the core region. Outside the core region, the light contrast suggests that the adsorbent layer is HDA. The inset of Figure 2b clearly demonstrates the interface between the crystalline Cu NWs. The presence of noticeable amorphous adsorbent layer was presumably responsible to high resistance due to the obstruction of contacts between NWs. It might have been removed by decomposition as a function of light to generate superior contact between Cu NWs.[45] The NWs were formed randomly without bundling and uniformly distributed over the substrate as shown in Figure 3. It revealed that, percolation was achieved in the Cu NW network based on the intersections of the NWs. Meanwhile, the Cu NWs network before sintering exhibited very weak connections between Cu NWs, leading to high contact resistance at the nanojunctions (Figure 3e and f).

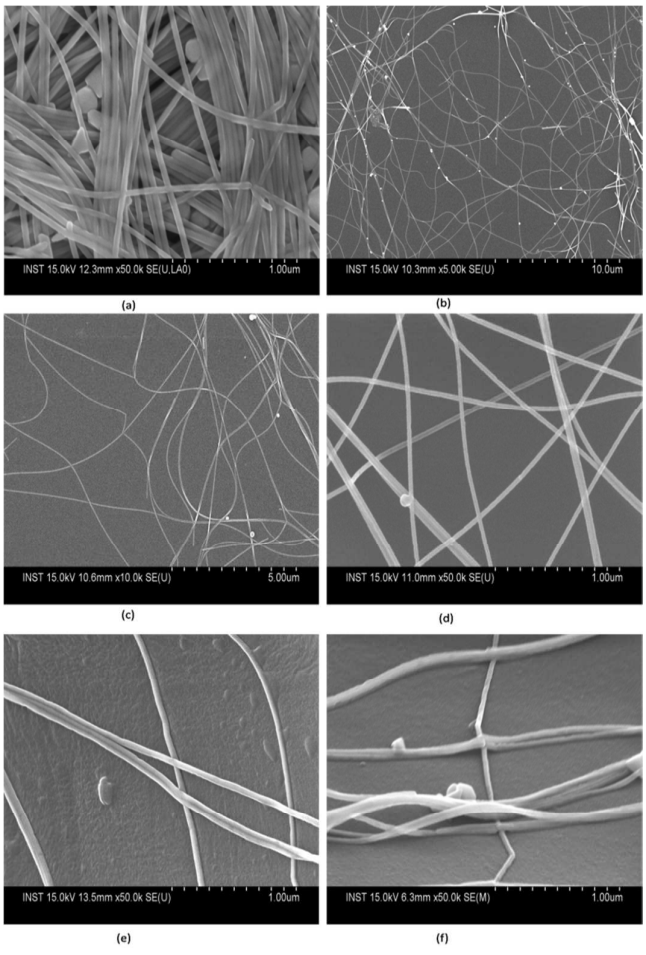

Figure 3: FE-SEM images of Cu NWs **(a)** Centrifuged nanowires **(b), (c)** and **(d)**Top view with different magnification, **(e)** and **(f)** Cross sectional view of Cu NWs on PET Substrate.

The optical transmittance of the fabricated Cu NW flexible transparent electrodes was measured, as depicted in Figure 4a. Series of Cu NW network TCEs were prepared by varying the

concentration of the Cu NW ink. The TCEs prepared using a lower volume (40 µl) of Cu NW ink displayed high optical transmission >95%. It was found that the sheet resistance and the transmittance of the solution-processed Cu NW network electrodes decreased with increasing concentration of the Cu NWs inks (Figure 4b and c).

The surface of Cu NWs is oxidized during their fabrication in water according to the following equations and the surface oxide/hydroxide hindrances electron conduction between the neighbouring NWs.

$$Cu^{2+} + 2OH^{-} \longrightarrow Cu(OH)_2$$

$$Cu^{2+} + 1/2(O_2) \longrightarrow CuO$$

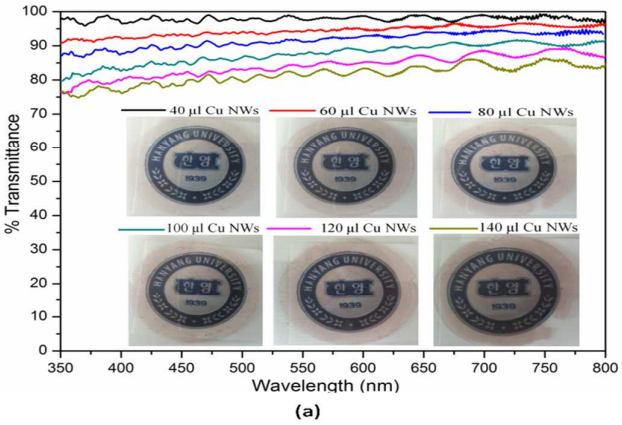

(a)

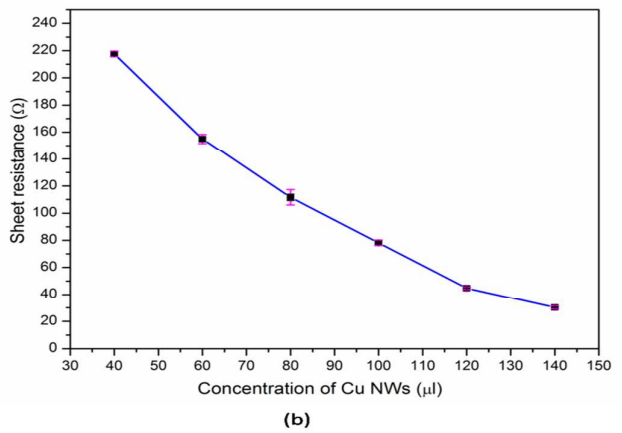

(b)

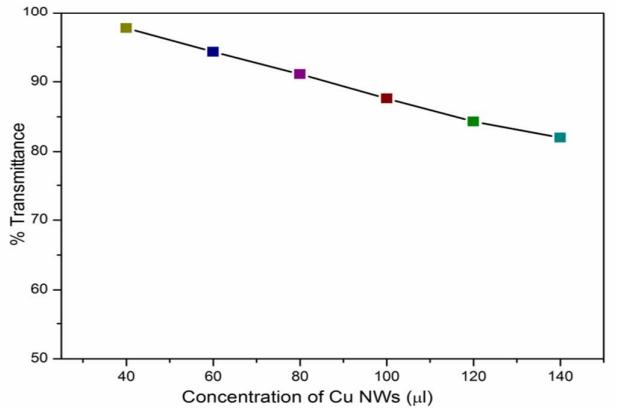

(c)

Figure 4: (a) Optical transmittance, **(b)** Variation of sheet resistance and **(c)** Variation of transmittance of electrodes as a function of concentration of Cu NW ink.

The residual HDA prevents the NWs from forming rigid contacts. It is difficult to completely remove the chemisorbed capping molecule, HDA, by general rinsing techniques. Post annealing at 250°C under an inert atmosphere is generally required to remove HDA, by which the NWs films become conductive.[46] In spite of the low sintering temperatures, conventional heating methods are still not friendly with common polymer foils, such as PET due to their low melting temperatures.[47, 48] Achieving a transmittance above 95% with a sheet resistance (Rs) less than100 Ω/□ using Cu NWs has been considered as a superior challenge.[49] To attain a high conductance, sintering of the percolation network is required to form the very small contact areas to wider necks, which should finally create dense conducting paths between the Cu NWs. To address these issues, we developed white flash light sintering method for welding of Cu NWs network. The WFL sintering method can instantly reduce the copper oxide shell and sinter copper nanostructures at room temperature while under ambient conditions in just time frame of 10^{-3} seconds without damaging the substrate. Moreover, a large area of Cu NW flexible electrode can be sintered by flash light from a xenon lamp with broad spectral range of visible region of irradiated light.[32] A schematic representation of the Cu NW welding procedure using a WFL system is shown in Figure 5.

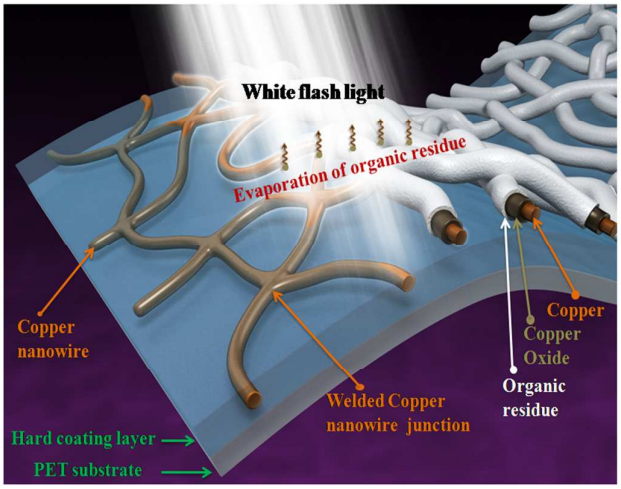

Figure 5: A schematic representation of white flash light welding process of percolated Cu NW network electrode.

To investigate the photonic welding characteristics of the percolated Cu NW networks, the flash light irradiation energy was varied from 1 to 3 J/cm^2 with a single 5 ms pulse. The sheet resistances of the percolated Cu NW networks were measured with respect to flash light irradiation conditions as shown in Figure 6a. The sheet resistance of the Cu NWs electrode was gradually decreased as the irradiation light energy increased to 3 J/cm^2 because neck-like junctions were formed successfully and they grew larger as the irradiation light energy increased (Figure 6b-f). It is noteworthy that the Cu NW network junctions could be welded and connected without the change of the morphology of the wires (Figure 6g).

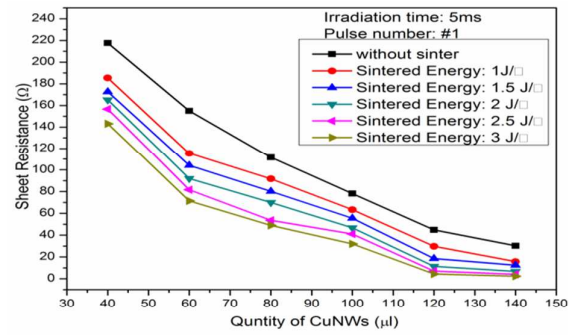

(a)

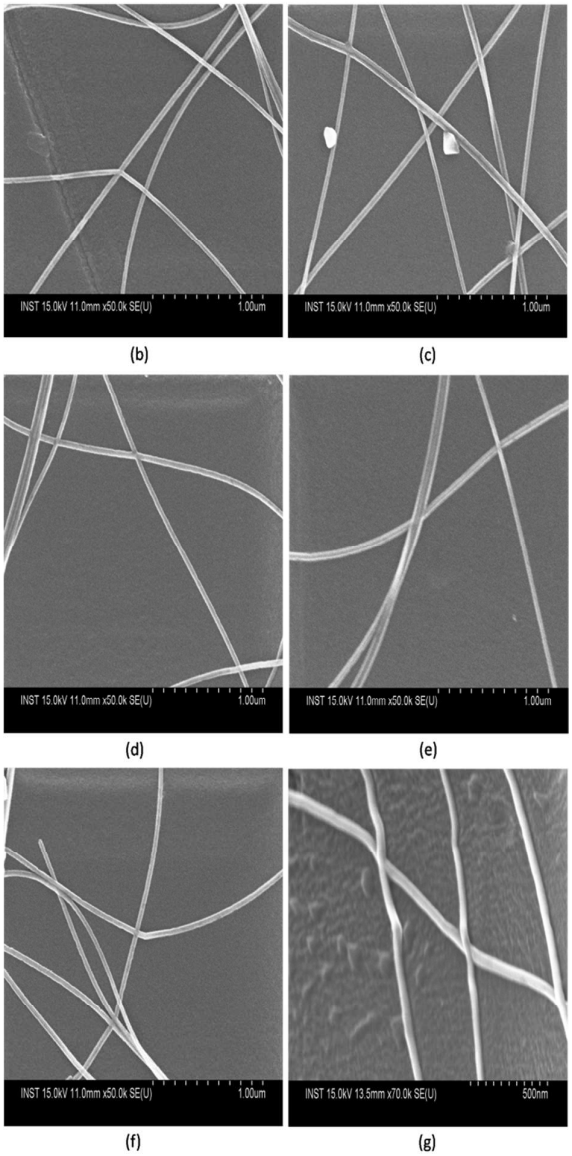

(b) (c) (d) (e) (f) (g)

Figure 6: (a) Variation of sheet resistance as a function of photonic energy. FESEM images of Cu NWs at different irradiation energy **(b)** 1 J/□, **(c)** 1.5 J/□, **(d)** 2 J/□, **(e)** 2.5 J/□, (**f**) 3 J/□, and **(g)** Cross sectional view FESEM images of photonic sintered (applied photonic energy=1J/□) Cu NWs at 40 µl concentration.

The Cu NWs could be welded at the junctions due to local heat generation derived from absorption of photonic energy according to the Zipper effect of metal nanowires.[20, 50] The pulse number of the WFL was increased from single to four pulses, and the sheet resistance of the Cu NW electrodes were measured (Figure 7a).The sheet resistances of the Cu NW electrodes gradually decreased as the number of pulses increased from one to four. This was because more total flash light energy was irradiated to the Cu NWs with increasing number of pulses which might have resulted in firm welding of Cu NWs and their neck-like junctions grew larger (Figure 7b, c, d and e). As shown in Figure 7, the Cu NWs were welded at the junctions due to local heat generated from absorption of photonic energy. However, if the number of pulses of the flash light irradiation was more than 4 pulses, Cu NW junctions were broken up due to the excessive irradiation energy after complete fusion of Cu NWs, resulting in a decrease in the number of current transport paths, as illustrated in Figure 7f. These results corroborate an increase in sheet resistance (Figure 7a).

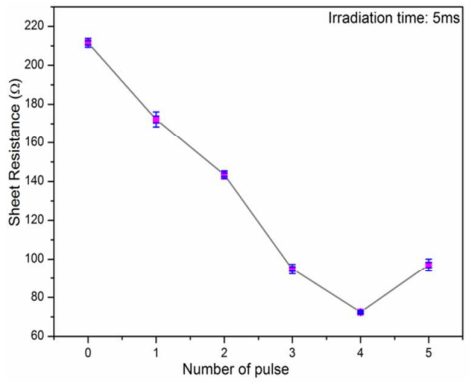

(a)

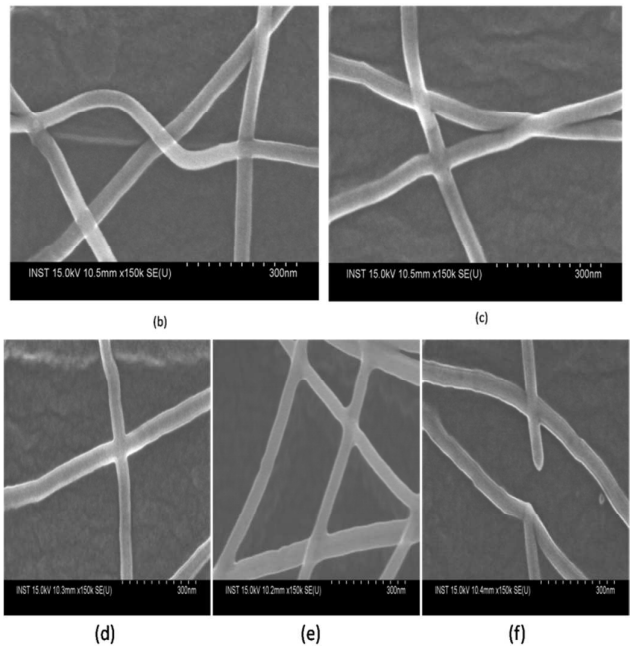

(b) (c) (d) (e) (f)

Figure 7: (a) Measurement of sheet resistance under variable pulse number. FE-SEM images of Cu NWs with variable pulse number **(b)** Pulse number: #1, **(c)** Pulse number: #2, **(d)** Pulse number: #3, **(e)** Pulse number: #4 and **(f)** Pulse number: #5

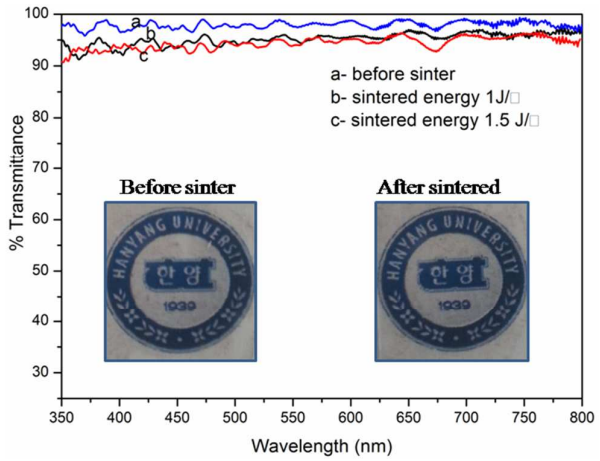

Figure 8: Optical transmittance spectra of Cu NWs (40 µl) ink before and after photonic sintered

Figure 8 shows the optical transmission spectra of the sintered Cu NW electrodes. The samples revealed high transmittance T > 95% at an irradiation energy of 1 J/cm^2 with one pulse. A 5 ms pulse duration seemed to be the optimal flash light sintering conditions required to obtain percolated Cu NW (40 µl) specimens. It was found that the transmittance was slightly decreased due to the welding of Cu NWs at the junctions on increasing the irradiation energy of flash light to 1.5 J/cm^2. The WFL sintering enables the welding of Cu NW networks without damage of the polymer substrate due to very short WFL pulses. However, in the case of highly transparent Cu NW network electrode, the absorption of sufficient light energy becomes more difficult since most of the photonic energy penetrates through the Cu NWs coated polymer substrate, which ultimately results in a faster increase in the local surface heat generation of the metal nanostructures to finish the sintering process. Obviously, heat conduction from the Cu NW network to the polymer substrate will tend to increase the temperature of the polymer substrate. Since it remarkably affects optical transparency of substrates, excessive heating and thermal damage can be prevented by applying the energy in pulses.[51, 52] In the optimal condition of pulse irradiation, the sheet resistance of the Cu NW electrode (40 µl) was decreased by about 37%(218.2 to 128 Ω/□).

Wide angle XRD measurements were conducted to determine the structure of the percolated Cu NWs on a PET substrate before and after WFL irradiation (Figure 9a). Bragg diffracted peaks were observed at 39.14°, 43.04°, and 50.2°, corresponding to the CuO (200), Cu(111) and Cu(200) facets of the Cu NWs.[53, 54] In metal nanostructures (such as Cu NWs) based flexible electrodes, the oxidative stability of the metal (like Cu) is an important issue for practical application. Many research groups are trying to circumvent these problems by adopting various methods including laser sintering method.[29] However, laser sintering method has several disadvantages like low speed, small spot sintering, high power and expensive maintenance of the sophisticated system. In order to overcome the aforementioned issues, photonic sintering method is well suited and it has more benefits such as large area sintering with reduction of oxide shell of copper surface. Upon photonic welding at 1J/cm^2, complete absence of the Cu oxide peaks was observed, and Cu became more crystalline, as the reflections appear to be more prominent in the XRD patterns (Figure 9b). These peaks suggest significantly narrower reflection than those corresponding to CuO, indicating that the Cu crystallite size became significantly larger due to the number of welded junctions. The crystalline growth of the welded Cu resulted in significant increase in the intensity of the (200) plane direction, which indicates the conversion of CuO to pure Cu. Therefore, it is noteworthy that the flash light irradiation completely reduced the oxide shells covering Cu NWs to pure Cu NWs.

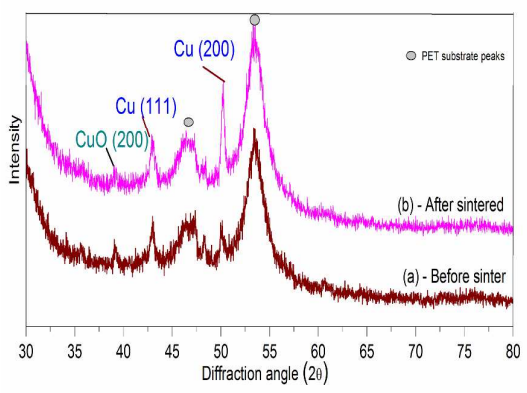

Figure 9: XRD spectra of before and after photonic sintering of Cu NWs on PET substrate

Recently, Nam et al. discovered that such alkyl amines could act like a long-chain alkyl groups and serve as a new class of reductant whose reducing power is active in the kinetically controlled reduction of CoO to Co nanoparticles.[55] Therefore, the same mechanism can be adopted without difficulty as an explanation for the copper oxide reduction mechanism in the present case. The possible chemical reactions that occur during WFL welding of the percolated Cu NW electrodes are as follows (Figure 10a). In this mechanism, the adsorbed HDA alkyl chains on the Cu NW might play a role as the reductant for the reduction of the CuO to pure Cu. The C-N bond cleavage of amines is known in photocatalytic hydrodenitrogenation reactions.[56,57] The subsequent reaction sequences are well-accepted reactions in organometallic chemistry, such as β-hydride elimination of the alkoxide, oxidative addition of C-H bonds, reductive elimination of NH_3 and $C_{16}H_{32}O$.[58,59] The surface hexadecyl species undergo β-H elimination to produce the hexadecanoic acid.[60, 61] Romeas et al. investigated the existence of intermediate formic, acetic acids and tetradecanoic acid during hexadecanoic acid photonic degradation by UV light irradiation using high-performance liquid chromatography (HPLC) and gas chromatography mass spectrometer (GCMS) analysis.[62] The temperature increase in the TCEs is caused by the adsorption of WFL with wavelengths ranging from 380 nm –1.0 µm by the Cu@ CuO structures. The WFL spectrum contains a large amount of visible region of light. The coated Cu NW network films are expected to adsorb a significant proportion of the energy supplied from the irradiation. Therefore, the nanowires absorb energies greater than or equal to the bandgap of CuO, promoting electrons across the bandgap.[63, 64] As the electrons relax to lower energy states, phonons are generated in the crystal lattice and cause a temperature rise in the material. The high intensity of the photons

creates a large number of phonons, which can elevate the temperature of the films from room temperature to several hundred degrees centigrade during the millisecond pulse.[65] Simultaneously, the photonic irradiation might have converted the alkyl chain to primary alcohols, secondary alcohols and carboxyl acid through photodegradation phenomena involving OH radical attack with O_2.[66,67]

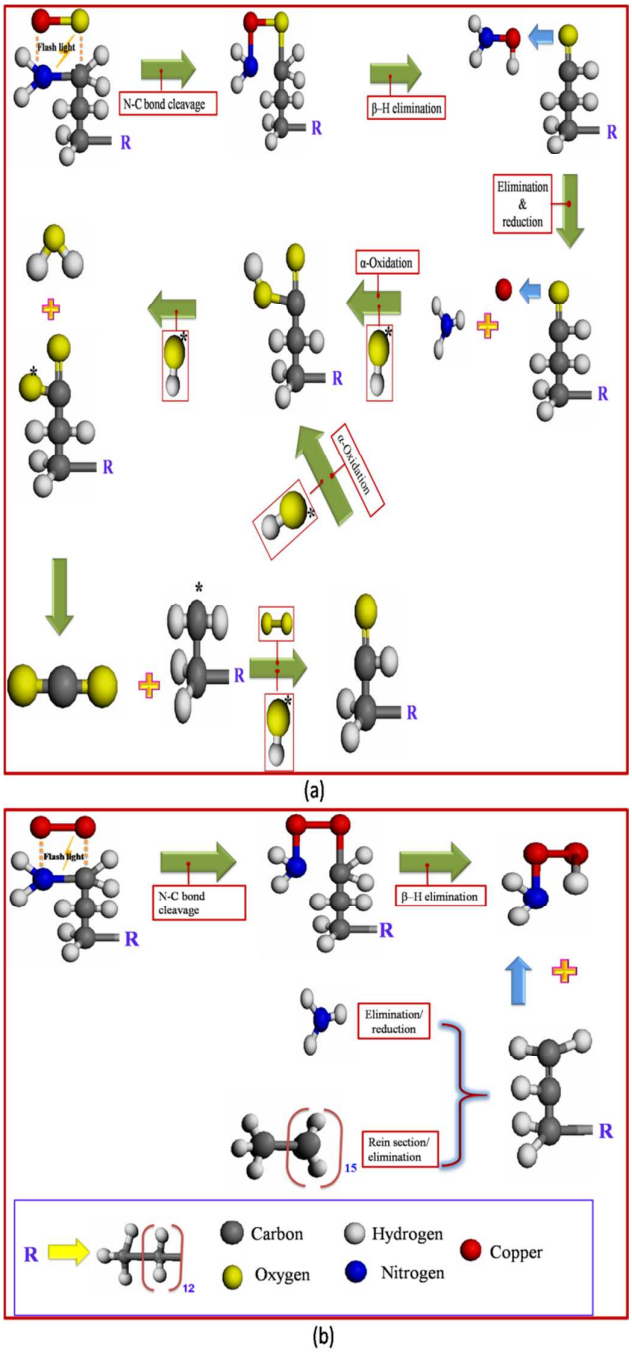

Figure 10: (a) Scheme 1: Proposed reaction pathway: reduction of CuO to Cu by HDA with decomposition mechanism under photonic irradiation. **(b) Scheme 2:** Conversion of HDA into Hexadecane and their photonic decomposition phenomena.

The high temperature of the Cu NWs may superheat their surface and generate energetic copper ions instantly. Therefore, the intermediate alcohol and acids resulting from photothermal degradation of HDA might reduce the copper oxide shell on the superheated Cu NWs. The XRD results clearly show that the absorbed HDA was decomposed and could play a role as the reductant to transform CuO to the pure Cu. The deamination of HDA followed by β-hydride and reductive eliminations of surface species on Cu proposed in Figure 10b would produce ammonia and hexadecane. The decomposition of hexadecane was explained by Ford, based on Fabuss, Smith and Satterfield mechanism.[34] The C_{16} radicals are produced mainly as secondary radicals and decompose by β-scission to give smaller alkyl radical and straight-chain alkenes. The alkyl radical, because of the high concentration of $C_{16}H_{34}$, preferentially abstracts hydrogen to give a straight-chain alkane and an alkyl radical that continues to decompose into CO_2 and H_2O.[68]

To investigate the in-depth phenomena, the vibrational spectra of the molecules adsorbed on the surfaces of the Cu NWs were investigated using characteristic transmittance peaks in FTIR spectroscopic studies. Figure 11 shows FTIR spectra in the region of 4000 - 400 cm^{-1} before and after WFL welding of Cu NWs. Vibrational peaks were observed at 3429, 2920, 2356, 1656, 1011-1404 and 538 cm^{-1}. The FTIR spectrum of the as-deposited films clearly showed the presence of organic residues, with peaks for the NH_2, C-H, C=O, and C-H bonds being observed (Figure 11a). The strong band at 3429 cm^{-1} is the N-H stretching band, which indicates binding of amine groups to the metal nanostructures. The peak at 2920 cm^{-1} corresponds to -C-H stretching of terminal -CH_3 and -CH_2 group of adsorbed HDA alkyl chains.[69] the strong peak at 2356 cm^{-1} is mostly due to the end-on coordination of C-N with the copper atoms at the surface of the obtained nanostructures.[70] The sharp peak at 1656 cm^{-1} is associated with scissoring mode of NH_2 vibrations. The stretching vibrations in the 1011-1404cm^{-1} range correspond to strong of strong C=O vibrations, carboxylic acids and alcohols and medium-to-strong C-N vibrations of amines.[71] FTIR analysis of the as-deposited Cu@CuO films was performed to understand the point at which the WFL treatment removed the organic residues from the electrodes. The films were subsequently treated with single pulse of light using an energy density of 1.0 J/cm^2, resulting in a significant reduction in the peak intensity for all of the bonds (Figure 11b).The absence of peaks in the corresponding FTIR spectrum indicated that the entire organic residue had been removed and thermally decomposed to form the reducing atmosphere. The peaks between 1000-1400 cm^{-1} are due to carboxylic acids, alcohols and residues of HDA, were removed by decomposition of the adsorbed HDA alkyl chains. The reduced peak at 2356 cm^{-1} is associated with dissociation of C-N with copper atoms at the surface of nanostructures. The decreased band at 2920 cm^{-1} corresponds to decomposition of -C-H stretchingterminal,-CH_3 and -CH_2 group of adsorbent alkyl chain of HDA. The increased bands at 1656 and 3429 cm^{-1} suggest that the attachment of -NH_2 group with copper atom at surface of NWs. Therefore, single pulse of light at this intensity appears to be sufficient for the electrode temperature to reach the decomposition temperature of the organic components surrounding the NWs. The decomposition products are acetone, formaldehyde, acetaldehyde and also include CO_2, C_2H_4 and H_2O.[68] Therefore, from the decomposition products of the organic residuals it is clear that OH^* is a key component of the reducing gases. Nevertheless, further optimization of the WFL process parameters (including energy, pulse number and duration time) is

required for the complete removal of the organic residues from the Cu NWs.

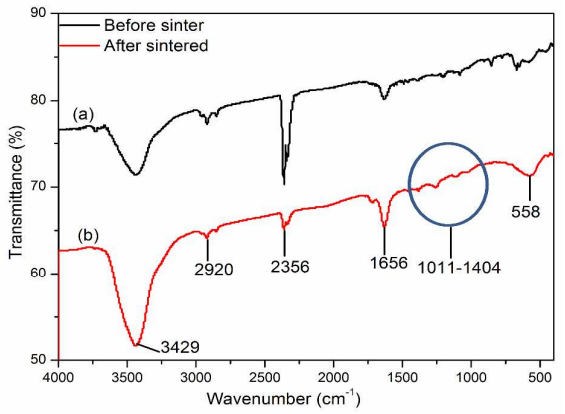

Figure 11: FTIR spectra of before and after photonic sintered Cu NWs.

Conclusions

In conclusion, we have demonstrated a hydrazine-free hydrothermal method for growing high aspect ratio Cu NWs. Photonic sintering using WFL provided a percolated Cu NWs network morphology with welded junctions due to local heat derived from the absorption of photonic energy according to the Zipper effect. We found that TCEs prepared using a low volume (40 µl) of ultra-long Cu NW ink exhibited an optical transmission of T >95%. The sheet resistance (R_S =128Ω/□) of the electrode decreased due to the photonic welding of wires enabling large interconnected networks. XRD results confirmed the absence of copper oxide and HDA after photonic sintering. WFL photonic sintering results in large-area welded metal nanostructured networks fabricated using an eco-friendly, simple and rapid sintering method. These TCEs can be used in printed and flexible display technologies.

Acknowledgements

This research was supported by Basic Science Research Program through the National Research Foundation of Korea (NRF) funded by the Ministry of Education (2012R1A6A1029029). This work was also supported by the Technology Innovation Program (or the Industrial Strategic Technology Development Program, 10048913, Development of cheap nanoink, which is sintered in air for smart devices) funded by the Ministry of Trade, Industry, & Energy (MI, Korea). This work was supported by Nano-Convergence Foundation (www.nanotech2020.org) funded by the Ministry of Science, ICT and Future Planning(MSIP, Korea) & the Ministry of Trade, Industry and Energy(MOTIE, Korea) [Project Number: R201502510]

Notes and references

1 C. Sachse, N. Weiß, N. Gaponik, L. Müller-Meskamp, A. Eychmüller, K. Leo, *Adv. Energy.Mater.*2014**, 4**, 1300737.
2 J. Lee, P. Lee, H. Lee, D. Lee, S. S. Lee, S. H.Ko, *Nanoscale*2012, **4**, 6408-6414.
3 C. Cheng, H. J. Fan, *Nano Today*2012, **7**, 327-343.
4 C. Sealy, C. *Nano Today* 2010,**5,** 507-511.
5 A. Kamyshny, S. Magdassi, *Small* 2014, **10**, 3515-3535.
6 Y. Jin, D. Deng, Y. Cheng, L. Kong, F. Xiao,*Nanoscale*2014, **6**, 4812-4818.
7 Z. Liu, J. Xu, D. Chen, G. Shen, *Chem. Soc. Rev.*2015, **44**, 161-192.
8 G. Gruner, *J. Mater. Chem.* 2006, **16**, 3533-3539.
9 D. S. Hecht, L. Hu, G. Irvin, G. *Adv. Mater*. 2011, **23**, 1482-1513.
10 Q. Cui, F. Gao, S. Mukherjee, Z. Gu, *Small* 2009, **5,** 1246-1257.
11 S. De, T. M. Higgins, P. E. Lyons, E.M. Doherty, P. N. Nirmalraj, W. J. Blau, J. J. Boland, J. N. Coleman, *ACS Nano*2009, **3,**1767-1774.
12 D. J. Lipomi, J. A. Lee, M. Vosgueritchian, B. C. K. Tee, J. A. Bolander, Z. Bao, *Chem. Mater.*2012**,24**, 373-382.
13 T. Tokuno, M. Nogi, J. Jiu, K. Suganuma, *Nanoscale Res. Lett.*2012, **7**, 281–285.
14 R.Zhu,C. H. Chung, K. C. Cha, W. Yang, Y. B. Zheng, H. Zhou, T. B. Song, C. C. Chen, P. S. Weiss, G. Li, Y. Yang. *ACS Nano* 2011, **5**, 9877-9882.
15 Y. Jiang, J. Xi, Z. Wu, H. Dong, Z. Zhao, B. Jiao, X. Hou, *Langmuir* 2015, **31**, 4950-4957.
16 Z. Q. Zheng, J. D. Yao, B. Wang, G. W. Yang, *Sci. Reports* 2015**,5**, 11070.
17 D. S. Hecht, L. Hu, G. Irvin, *Adv. Mater.* 2011, **23**, 1482–1513.
18 S. Kiruthika, R. Gupta, K. D. M. Rao, S. Chakraborty, N. Padmavathy, G. U. Kulkarn, *J. Mater. Chem. C*, 2014, **2**, 2089–2094.
19 H. Zhu, Z. Fang, C. Preston, Y. Li, L. Hu, *Energy Environ. Sci.* 2014, **7**, 269-287.
20 E. C. Garnett, W. Cai, J. J. Cha, F.Mahmood, S. T. Connor, M. G. Christoforo, Y. Cui, M. D. McGehee, M. L.Brongersma, *Nat. Mater.* 2012,**11**, 241-249.
21 J. Y. Lee, S. T. Connor, Y. Cui, P. Peumans,*Nano Lett.*2008, **8**, 689-692.
22 U. S. Geological Survey, Mineral Commodity Summaries. 2015, 1-195.
23 A. R. Rathmell, B. J. Wiley, *Adv. Mater.*2011, **23**, 4798-4803.
24 S. Bhanushali, P. Ghosh, A. Ganesh, W. Cheng, *Small* 2015, **11**, 1232-1252.
25 W. H. Xu, L. Wang, Z. Guo, X. Chen, J. Liu, X. J. Huang, *ACS Nano* 2015, **9**, 241-250.
26 J. W. Liu, H. W. Liang, S. H. Yu, *Chem. Rev.*2012, **112**, 4770-4799.
27 J. Perelaer, B. J. de Gans, U. S. Schubert, *Adv. Mater.*2006, **18,** 2101–2104.
28 S. Wunscher, R. Abbel, J. Perelaer, U. S. Schubert, *J. Mater. Chem. C.* 2014**,2**, 10232-10261.
29 S. Han, S. Hong, J. Ham, J. Yeo, J. Lee, B. Kang, P. Lee, J. Kwon, S. S. Lee, M. Y. Yang, S. H. Ko, *Adv. Mater.*2014, **26**, 5808–5814.
30 H.-S. Kim, S. R. Dhage, D.-E. Shim and H. T. Hahn, *Applied Physics A*, 2009, **97**, 791-798.
31 J. Ryu, H.-S. Kim and H. T. Hahn, *Journal of Electronic Materials*, 2011, **40**, 42-50.
32 H.-J. Hwang, W.-H. Chung and H.-S. Kim, *Nanotechnology*, 2012, **23**, 485205.
33 S.-J. Joo, H.-J. Hwang and H.-S. Kim, *Nanotechnology*, 2014, **25**, 265601.
34 Y.-J. Kim, C.-H. Ryu, S.-H. Park and H.-S. Kim, *Thin Solid Films*, 2014, **570**, 114-122.
35 W.-H. Chung, H.-J. Hwang and H.-S. Kim, *Thin Solid Films*, 2015, **580**, 61-70.
36 H.-J. Hwang, S.-J. Joo and H.-S. Kim, *ACS applied materials & interfaces*, 2015, **7**, 25413-25423.
37 Y. Won, A. Kim, D. Lee, W. Yang, K. Woo, S. Jeong, J. Moon, *NPG Asia Materials* 2014,**6**, e105.
38 J. S. Kang, J. Ryu, H. S. Kim, H. T. Hahn, *J. Electro. Mater.*2011,**40**, 2268-2277.

39 M. Jin, G. He, H. Zhang, J. Zeng, Z. Xie, Y. Xia, *Angew.Chem.Int.Ed.*2011,**50**, 10560-10564
40 M. Kevin, G. Y. R. Lim, G. W. Ho, *Green Chem*.2015**,17**, 1120-1126.
41 M.Mohl, P. Pusztai, A.Kukovecz, Z. Konya, *Langmuir*2010,**26**, 16496-16502.
42 A. K. Ganguli, A. Ganguly, S. Vaidya, *Chem. Soc. Rev.*2010, **39**, 474–485.
43 M. H. Wood, R. J. L. Welbourn, T. Charlton, A. Zarbakhsh, M. T. Casford, S. M. Clarke, *Langmuir*2013**, 29**, 13735-13742.
44 Y. Zhao, Y. Zhang, Y. Li, Z. Yan, *New. J. Chem.*2012**, 36,**130-138.
45 Y. Chen, C. Hu, X. Hu, J. Qu, *Environ. Sci. Technol*. 2009, **43**, 2760–2765.
46 D. Zhang, R. Wang, M. Wen, D. Weng, X. Cui, J. Sun, H. Li, Y. Lu,*J. Am. Chem. Soc.*2102, **134,** 14283-14286.
47 J. Perelaer, M. Klokkenburg, C. E. Hendriks, U. S. Schubert,*Adv. Mater.* 2009, **21**, 4830–4834.
48 S. Bae, H. Kim, Y. Lee, X. Xu, J. S. Park, Y. Zheng, J. Balakrishnan, T. Lei, H. R. Kim, Y. Il Song, Y. J. Kim, K. S. Kim, B. O. Zyilmaz, J. H. Ahn, B. H. Hong, S. Iijima, *Nature Nanotechnology* 2010**, 10**, 574-578.
49 J. Song, J. Li, J. Xu, H. Zeng, *Nano Lett.*2014**,14**, 6298−6305.
50 Y. Sun, S. Jin, G. Yang, J. Wang, C. Wang, *ACS Nano* 2015, **9**, 3479-3490.
51 S. B. Yang , H. K. Choi , D. S. Lee , C.G. Choi , S. Y. Choi , Il-Doo Kim*, Small*2015, ***11***, 1293–1300.
52 H. Y. Yang,J. M. Hong,T. W. Kim, Y. W. Song, W. K. Choi, J. A. Lim, *ACS Appl. Mater. Interfaces*2014, **6**, 1495−1501.
53 D. V. R. Kumar, I. Kim, Z. Zhong, K. Kim, D. Lee, J. Moon, *Phys. Chem. Chem. Phys.*2014**, 16**, 22107-22115.
54 X. Liu, B. Geng, Q. Du, J. Ma, X. Liu, *Mater. Sci. Eng. A.* 2007, **448**, 7–14.
55 K. M. Nam, J. H. Shim, H. Ki, G. Sang-Il Choi, Lee, J. K. Jang, Y. Jo, M. H. Jung, H. Song, J. T. Park,*Angew. Chem. Int. Ed.*2008,**47**, 9504–9508.
56 J. L. Portefaix, M. Cattenot, M. Guerriche, M. Breysse, *Catal. Lett.* 1991, **9**, 127-132.
57 N. Iqbal, E. J. Cho, *Adv. Synth. Catal.*2015,**357**, 2187 – 2192.
58 S. Mourdikoudis, L. M. Liz-Marzan, *Chem. Mater.* 2013, **25,** 1465−1476.
59 H. Sun, X. Jiao, H. Wang, Z. Jiang, D. Chen, *ACS Appl. Mater. Interfaces*2011, **3,** 2425–2430.
60 R. Atkinson, *Int. J. Chem. Kinetics*, 1997, **29**, 99–111.
61 U. Scheller, T. Zimmer, D.Becher, F. Schauer, W. H. Schunck, *The J. Biological Chem.*1998,**273,** 32528–32534.
62 V. Romeas, P. Pichat, C. Guillard, T. Chopin, C. Lehaut,*New J. Chem.*1999,**23**, 365-373
63 M. Jha, R. Dharmadasa, G. L. Draper, A. Sherehiy, G. Sumanasekera, D. Amos, T. Druffel, *Nanotechnology*, 2015,**26,** 175601.
64 M. S. Brown, C. B. Arnold,*Springer Series in Materials Science* 2010, **135**, 91-120.
65 F.Hassouna, S. Therias, G. Mailhot, J. L. Gardette, *Polymer Degradation and Stability,* 2009**,94**, 2257–2266
66 R. Atkinson, *Atmos. Environ. A* 1990, **24,** 1-41.
67 T. J. Ford, *Ind. Eng. Chem. Fundam.*1986, **25**, 240-243
68 B.Peng, C. Zhao, S. Kasakov, S. Foraita, J. A. Lercher, *Chem. Eur. J.* 2013, **19**, 4732 – 4741.
69 F. Yu, X. Xu, C. J. Baddeley, R. M. Bellabarba, P. Lignier, R. P. Tooze, F. Fina, J. S. T. Irvine, W. Zhou, *Cryst. Eng. Comm.*2014, **16**, 1714-1723.
70 T. Mishra, R. K. Sahu, S. H. Lim, L. G. Slamanca-Riba, S. Bhattacharjee,*Mater. Chem. Phy.* 2010**, 123**, 540-545.
71 J. K. Cooper, A. M. Franco, S. Gul, C. Corrado, J. Z. Zhang, *Langmuir* 2011, **27**, 8486-8493.